Corrosion of $Al_{0.1}CoCrFeNi$ High Entropy Alloy in a Molten Eutectic Salt

JES Focus Issue on Advanced Techniques in Corrosion Science in Memory of Hugh Isaacs

Corrosion of $Al_{0.1}CoCrFeNi$ High Entropy Alloy in a Molten Eutectic Salt

A. A. Jalbuena,[1] Nicholas Ury,[1] Jaewan Bae,[1] Christopher Faraj,[1] Kailey Hanan,[1] Shahan Kasnakjian,[1] J. K. Logier,[1] R. S. Mishra,[2] X. Wang,[3] J. C. Earthman,[3,z] and V. Ravi[1,*]

[1] *Department of Chemical and Materials Engineering, California State Polytechnic University, Pomona, California, USA*
[2] *Department of Materials Science and Engineering, University of North Texas, Denton, Texas, USA*
[3] *Department of Materials Science and Engineering, University of California, Irvine, California, USA*

The present work investigates the hot corrosion behavior of $Al_{0.1}CoCrFeNi$ high entropy alloy (HEA) and Ni-base Alloy 718. Electrochemical tests were conducted to characterize the corrosion behavior of $Al_{0.1}CoCrFeNi$ HEA and Alloy 718 in a molten Na_2SO_4-NaCl eutectic mixture at 750 ± 5°C in the presence of a platinum catalyzed SO_2/air mixture. The morphology of the surface of $Al_{0.1}CoCrFeNi$ HEA and Alloy 718 was investigated using scanning electron microscopy (SEM) as well as energy dispersive spectroscopy (EDS). The results indicate that the polarization resistance of the HEA was higher and the corrosion rate lower in comparison with Alloy 718. SEM and EDS analyses reveal the formation of a dual oxide layer on the HEA that provides a better corrosion barrier compared to the single chromia scale observed on Alloy 718.
 [DOI: 10.1149/2.0561911jes]

Manuscript submitted March 25, 2019; revised manuscript received June 13, 2019. Published July 17, 2019. *This paper is part of the JES Focus Issue on Advanced Techniques in Corrosion Science in Memory of Hugh Isaacs.*

Compositionally complex high entropy alloys (HEAs) have emerged as attractive candidate materials for advanced engineering applications due to their unique microstructures and mechanical properties. Unlike traditional alloys, HEAs contain five or more elements with equal or near-equal amounts (in atom %).[1,2] This unconventional alloying (Figure 1) strategy results in HEAs with attractive properties, e.g., wear resistance, hardness and high temperature strength coupled with relatively low density and multiple elements that could participate in passive film formation. The random arrangement of multiple elements in solid solutions results in a particular locally-disordered chemical environment, which is expected to result in unique properties.[3] However, the literature is sparse in regard to the stability of these alloys in corrosive environments, e.g. in molten salts. In gas turbine environments, salts can deposit on the turbine blade forming a thin molten film, which will induce hot corrosion.[4] The corrosive salts will attack the protective oxides, forcing the substrate to undergo further degradation.[5] Therefore, it is important to evaluate the corrosion resistance of these alloys to determine their suitability for service under these conditions. The aim of the present work was to evaluate the corrosion behavior of an $Al_{0.1}CoCrFeNi$ HEA in a molten salt environment and benchmark it to a conventional Ni-base superalloy, Alloy 718, that is used in aircraft engines.

Experimental

HEA coupons of $Al_{0.1}CoCrFeNi$ were obtained from Sophisticated Alloys Inc. The HEA was vacuum induction melted and cast. The control alloy was Alloy 718 (Haynes International). The composition of these two alloys (in at%) are listed in Table I.

$Al_{0.1}CoCrFeNi$ HEA and Alloy 718 samples were electrochemically tested at 750 ± 5°C in a Na_2SO_4-NaCl eutectic mixture as the electrolyte. The electrochemical cell consisted of three electrodes positioned inside an alumina crucible. Tests were conducted in the presence of a platinum catalyzed SO_2/air mixture. Pure platinum wire was used for both the reference and counter electrodes. The working electrode was fabricated using coupons ground to a 600-grit surface finish. Electrochemical tests were conducted using a commercially available potentiostat.[6] The testing procedure involved recording the open circuit potential (OCP) for one hour. This was followed by a linear polarization (LP) scan from −20 to +20 mV relative to the OCP at a scan rate of 1 mV/s. Following this, a cyclic potentiodynamic polarization (CPP) scan was conducted from −400 to +400 mV relative to the OCP at a rate of 1 mV/s. After exposure to the molten salt environment, the test specimens were electroplated with nickel to help retain the corrosion product, and then epoxy mounted. The test coupons were metallographically prepared to a 1 μm surface finish and analyzed using scanning electron microscopy (SEM) coupled with energy dispersive spectroscopy (EDS).

Results and Discussion

The average OCP values recorded at the 60th minute are −897 ± 39 mV (N = 3, where N represents the number of replicates) and −701 ± 227 mV (N = 4) for the HEA and Alloy 718, respectively. The OCP trends as a function of time indicated that the alloys stabilized within the 60 minute time frame. The polarization resistance, R_p (Ω cm^2), can be used as a measure of corrosion resistance, i.e.,

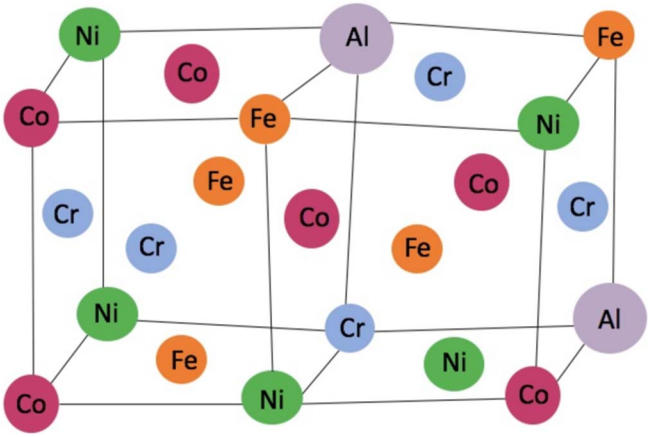

Figure 1. Schematic depiction of an HEA crystal lattice.

*Electrochemical Society Member.
[z]E-mail: earthman@uci.edu

Table I. Composition of the HEA and Alloy 718 (in at%).

	Ni	Cr	Fe	Co	Al	Mo	Ti	Nb + Ta	Density (g/cm^3)
HEA	24.40	24.45	24.40	24.35	2.4	-	-	-	7.66
Alloy 718	51.76	20.22	19.88	0.99*	1.08	1.83	1.10	3.14	8.20

*max.

a higher value of R_p indicates higher corrosion resistance. R_p values are obtained by determining the slope of the tangent at zero current density. Linear polarization plots for $Al_{0.1}$CoCrFeNi HEA and control Alloy 718 samples at 750°C are illustrated in Figure 2. The average R_p values for the HEA and Alloy 718 are 143 ± 69 (N = 3) and 91 ± 60 (N = 4) Ωcm^2, respectively. Therefore, the HEA has a higher corrosion resistance than Alloy 718 in Na_2SO_4-NaCl molten salt environments. The open circuit potential from the LPR plot for the HEA was −903 ± 34 mV (N = 3) and that for Alloy 718 was −709 ± 229 mV (N = 4). Corrosion current densities, i_{corr} (μA/cm^2), can be used to calculate the corrosion rate (mils per year, mpy) assuming uniform corrosion. Figure 3 shows the CPP plots for $Al_{0.1}$CoCrFeNi HEA and Alloy 718. Commercial software (EC-Lab) was used to calculate corrosion potential values and the corrosion current densities using the Tafel extrapolation method.[7–9] Regression lines were fitted to the linear portions of the cathodic and anodic sections of the initial portion of the potentiodynamic plot (−400 mV to 0 mV and 0 mV to +400 mV from OCP) and extrapolated until they intersected. This point of intersection defines the corrosion potential and the corrosion current density which was then used to calculate corrosion rates using Equation 1. The corrosion potentials for the HEA and Alloy 718 are −1116 ± 136 mV (N = 3) for HEA and −998 ± 276 mV (N = 4), respectively.

The equation for uniform corrosion rate is displayed below.

$$Corrosion\ Rate\ =\ 0.13\times\frac{i_{corr}}{\rho}\times EW \qquad [1]$$

where ρ is density of the alloy (g/cm^3) and EW is equivalent weight (gram equivalent) of the alloy.

The HEA exhibited a lower corrosion rate [31 ± 34 (N = 3) mpy] than Alloy 718 [90 ± 39 (N = 4) mpy]. The lower corrosion rate for the HEA can be attributed to the higher chromium activity relative to Alloy 718. This finding is consistent with results reported in the literature.[10] It is important to note that performing cathodic and anodic scans in succession and/or sweeping the potential over large ranges (± 0.4 V versus OCP) can alter the surface of the test coupon and the corresponding test results. It can be seen in Figure 3 that the corrosion potentials of both alloys are significantly lower than those in Figure 2. This difference is likely due to the large overpotentials used in the cyclic polarization scans. However, Alloy 718 continued to exhibit higher nobility than HEA ($Al_{0.1}$CoCrFeNi). The large potential range used in the present study ensures that all corrosion behavior is captured in the scans (i.e., multiple corrosion potentials, active/passive behavior and localized attack), which would otherwise be missing in a scan over small potential ranges (± 0.25 V versus OCP).

Figure 4 shows a backscattered electron image and corresponding EDS maps of the cross-section of an HEA coupon exposed to molten Na_2SO_4-NaCl at 750°C. The SEM image and the corresponding elemental maps indicate the formation of two distinct oxide layers, i.e., an outer chromium oxide and an inner aluminum oxide layer. The other constituent elements of the HEA, cobalt, iron and nickel, were not present in these oxide layers. Figure 5 shows a higher magnification backscattered electron image and corresponding EDS maps of the same cross-sectioned HEA coupon as above. At this magnification, the dual oxide layer can be more clearly seen. Additionally, a distinctly different region exists beneath the alumina film. This region is depleted of chromium and enriched in cobalt, nickel and iron. The compositions of selected points are provided in Table II and the significance of these points is discussed below.

Figures 6–9 show backscattered electron images and elemental maps of the cross-section of Alloy 718 coupons exposed to molten Na_2SO_4-NaCl at 750°C. A porous outer layer containing niobium, chromium, aluminum and oxygen and a denser inner layer of chromium oxide are apparent from these figures. Underneath the chromia layer, a region rich in niobium, aluminum and sulfur was observed. Beneath this, niobium sulfide particles embedded in a metallic matrix consisting primarily of nickel and iron was observed.

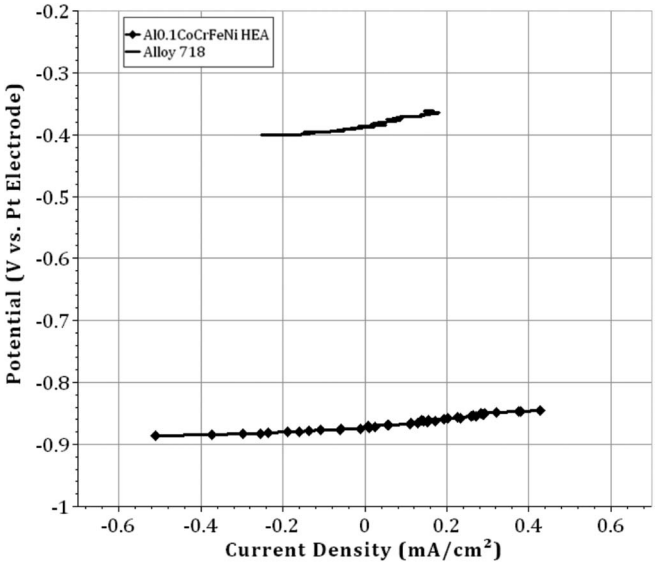

Figure 2. Representative linear polarization plots for $Al_{0.1}$CoCrFeNi HEA and Alloy 718 at 750°C in Na_2SO_4-NaCl.

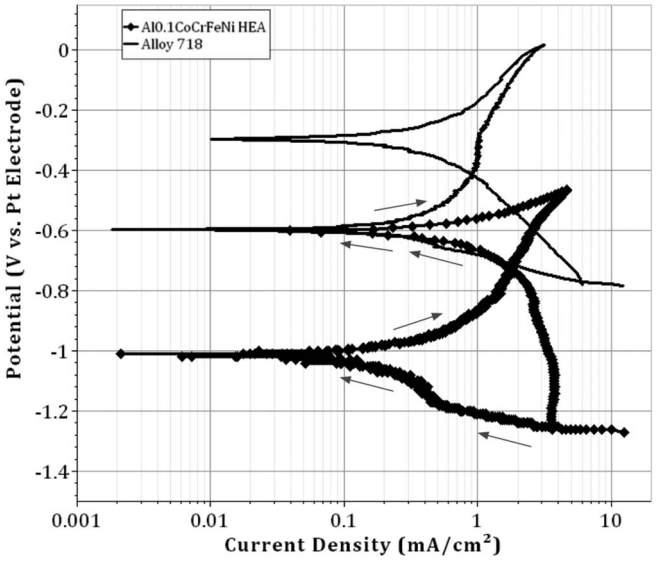

Figure 3. Representative cyclic potentiodynamic polarization plots for samples tested at 750°C in Na_2SO_4-NaCl. Arrows indicate the direction of the scan.

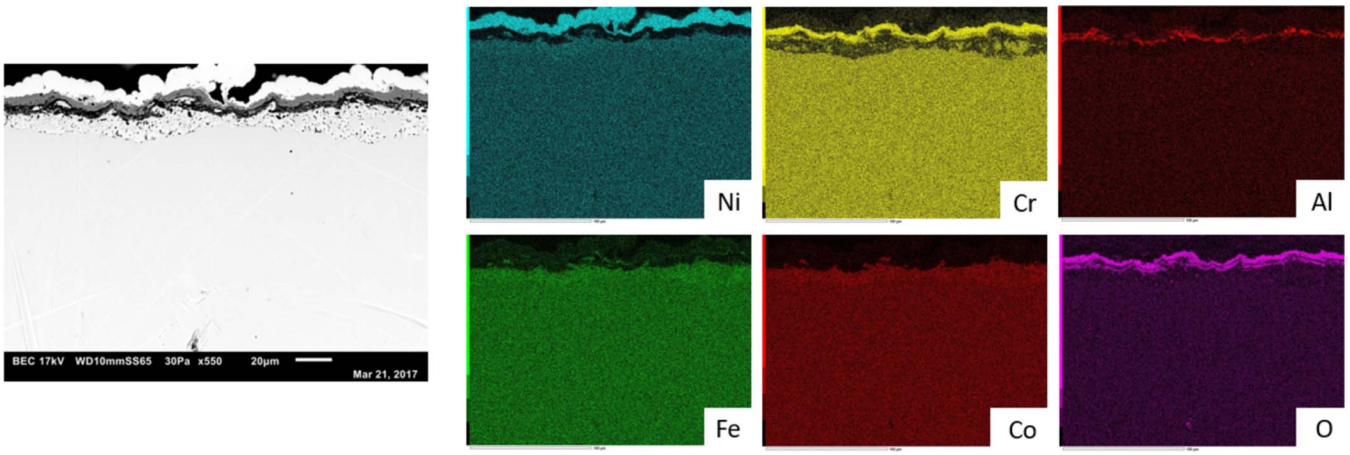

Figure 4. Backscattered electron image and corresponding EDS elemental maps of cross-sectioned $Al_{0.1}CoCrFeNi$ HEA sample exposed at 750°C in Na_2SO_4-NaCl at the surface.

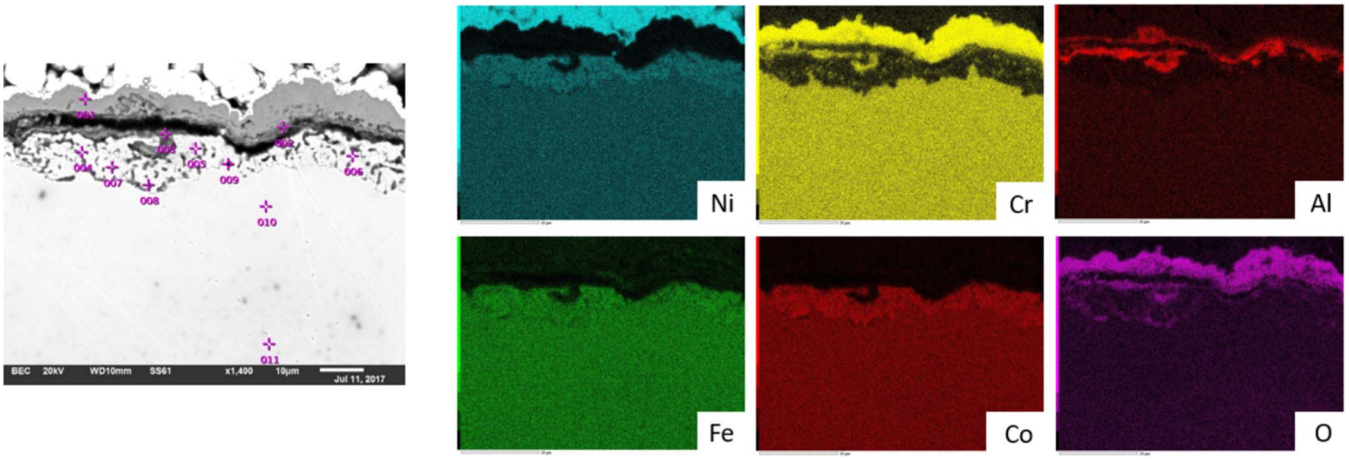

Figure 5. Higher magnification backscattered electron image and corresponding EDS elemental maps of cross-sectioned $Al_{0.1}CoCrFeNi$ HEA sample exposed at 750°C in Na_2SO_4-NaCl.

The present study has shown that $Al_{0.1}CoCrFeNi$ HEA forms an outer chromium oxide layer and an inner aluminum oxide layer when exposed to molten Na_2SO_4-NaCl. The presence of a dual oxide film on an HEA immersed in molten Na_2SO_4-NaCl salt has been observed on an AlCoCrFeNiTi HEA at 900°C.[5] In addition, the cross-sectional morphology of the $Al_{0.1}CoCrFeNi$ alloy used in this study is comparable to that of the corrosion behavior of AlCoCrFeNiTi alloy reported in the literature.[5] The Cr_2O_3 film is beneficial in defending against hot corrosion attack by modifying the ionic character of the electrolyte, i.e., by the formation of compounds such as $NaCrO_2$, Na_2CrO_4 and $Na_2Cr_2O_7$.[12] This dissolution of Cr_2O_3 will result in a positive solubility gradient that can interrupt the corrosion process at elevated temperatures.[12] The presence of an alumina film has been reported to be beneficial in several alloy systems because it can extend the initiation stage of hot corrosion as well as delay the propagation stage.[13]

Table II. Composition (in at%) of points listed on backscattered electron image shown in Figure 5.

	Element					
Point ID	Al	Co	Cr	Fe	Ni	O
1	-	-	35.53	2.41	9.71	52.34
2	31.85	1.40	16.07	2.08	2.93	45.67
3	33.13	2.64	13.69	2.13	3.82	44.6
4	-	31.44	4.71	23.64	31.64	8.57
5	-	29.12	2.09	23.34	32.13	13.33
6	-	29.99	2.45	23.42	30.48	13.66
7	-	26.69	3.39	18.21	24.85	26.86
8	-	24.21	8.60	18.44	23.28	25.47
9	-	27.67	8.49	21.49	28.76	13.59
10	3.72	23.14	22.11	22.10	22.60	6.33
11	3.21	21.51	20.66	20.84	21.88	11.90

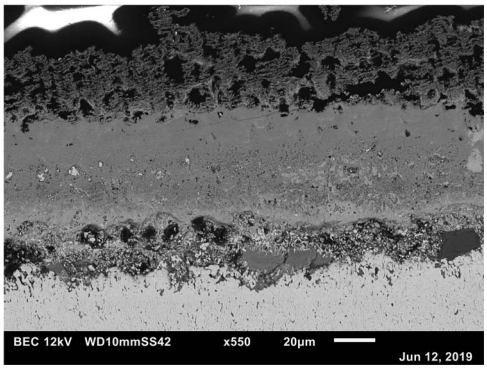

Figure 6. Backscattered electron image of cross-sectioned Alloy 718 sample exposed at 750°C in Na_2SO_4-NaCl.

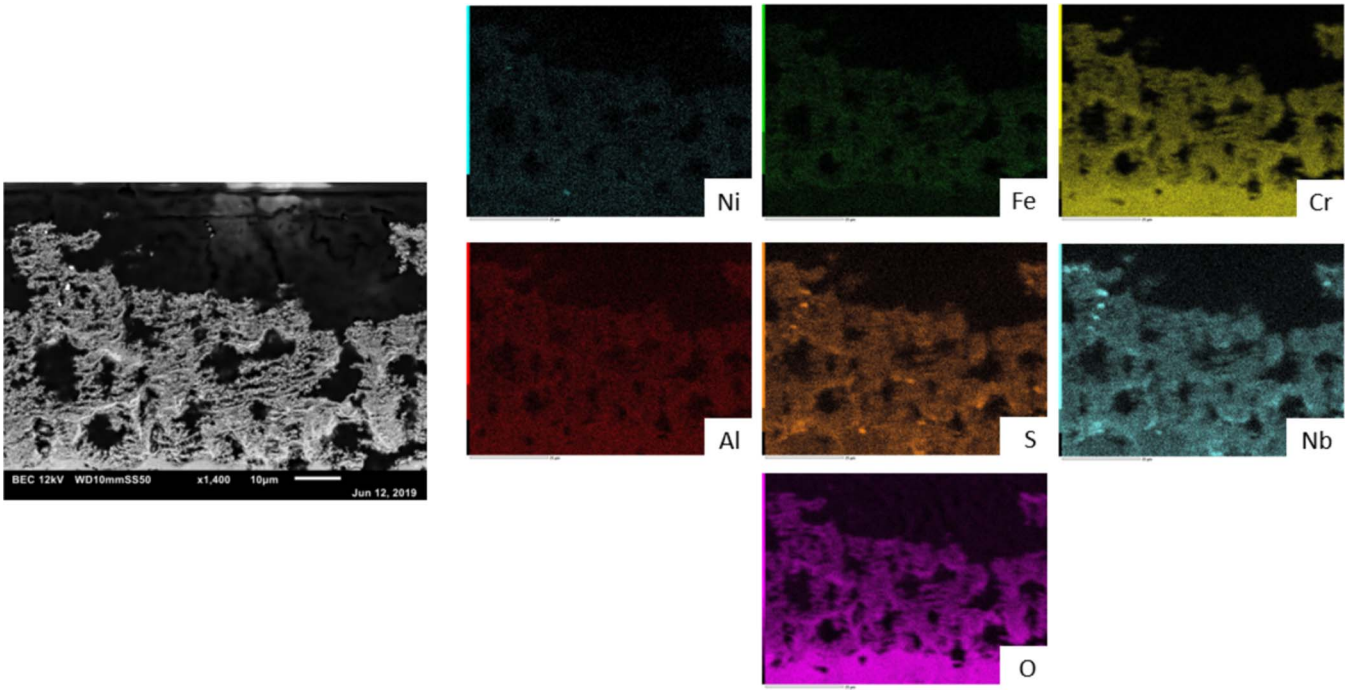

Figure 7. Higher magnification backscattered electron image and corresponding EDS elemental maps of the outer (porous) layer shown in Figure 6.

From Table II, the compositions of several points in Figure 5 are presented. These point analyses indicate that the oxide film has an outer region enriched in chromium and oxygen, indicating chromia, and the inner region is enriched in aluminum and oxygen indicating alumina. Some chromium is present in the alumina film. Beneath the oxide layer, chromium and aluminum are depleted. This depletion zone thickness is in the 5–10 μm range. The chromium and aluminum contents increase going into the substrate until they reach the pre-test composition deep into the substrate. This depletion zone is formed by the outward diffusion of aluminum and chromium. The depletion of chromium underneath the alumina film may be an issue if both the chromia and alumina films are ruptured after long exposures to the molten salts, as there will not be enough chromium at the surface to heal the chromia film. The ability of the HEA to form a dual oxide layer suggests that while the outer chromia layer provides an effective defense against the molten salt, the inner alumina layer could serve as a secondary barrier in protecting the underlying substrate.

Alloy 718 develops a single chromium oxide layer upon exposure to molten Na_2SO_4-NaCl at 750°C. The formation of an outer chromia layer for Alloy 718 in similar salts has been observed.[14,15] Sulfides can

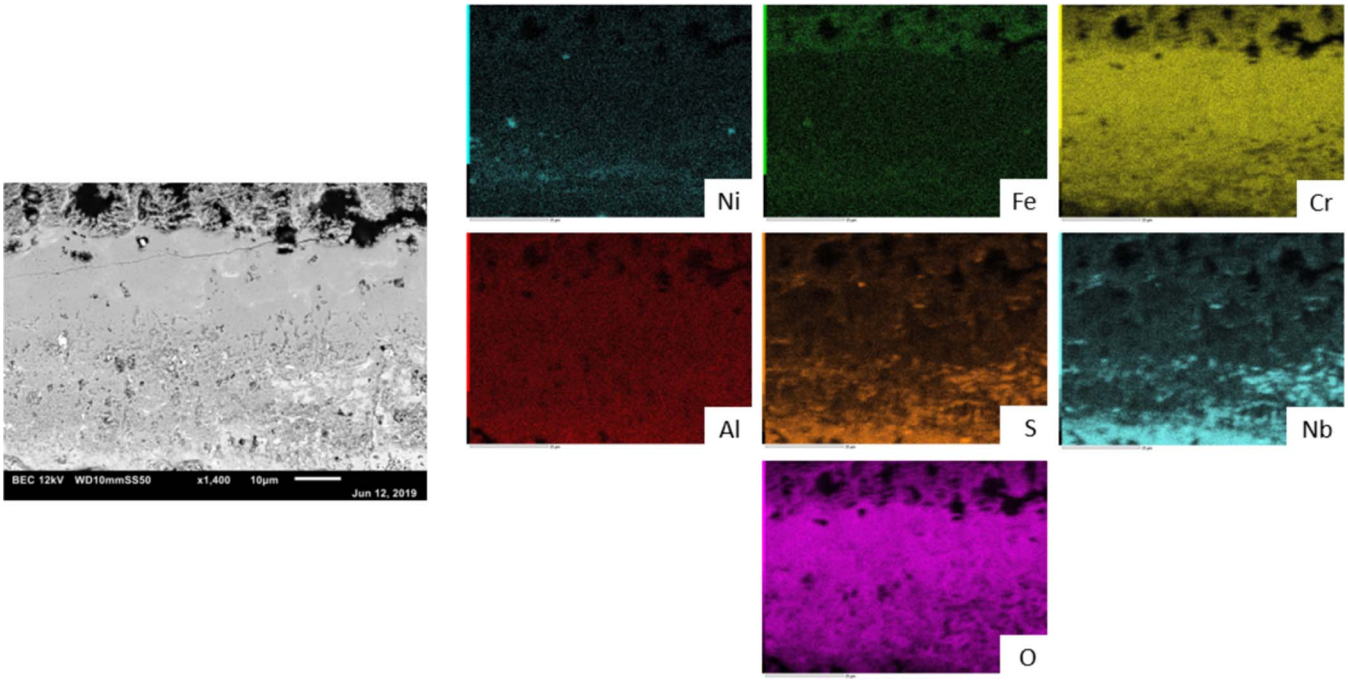

Figure 8. Higher magnification backscattered electron image and corresponding EDS elemental maps of the middle (dense) layer shown in Figure 6.

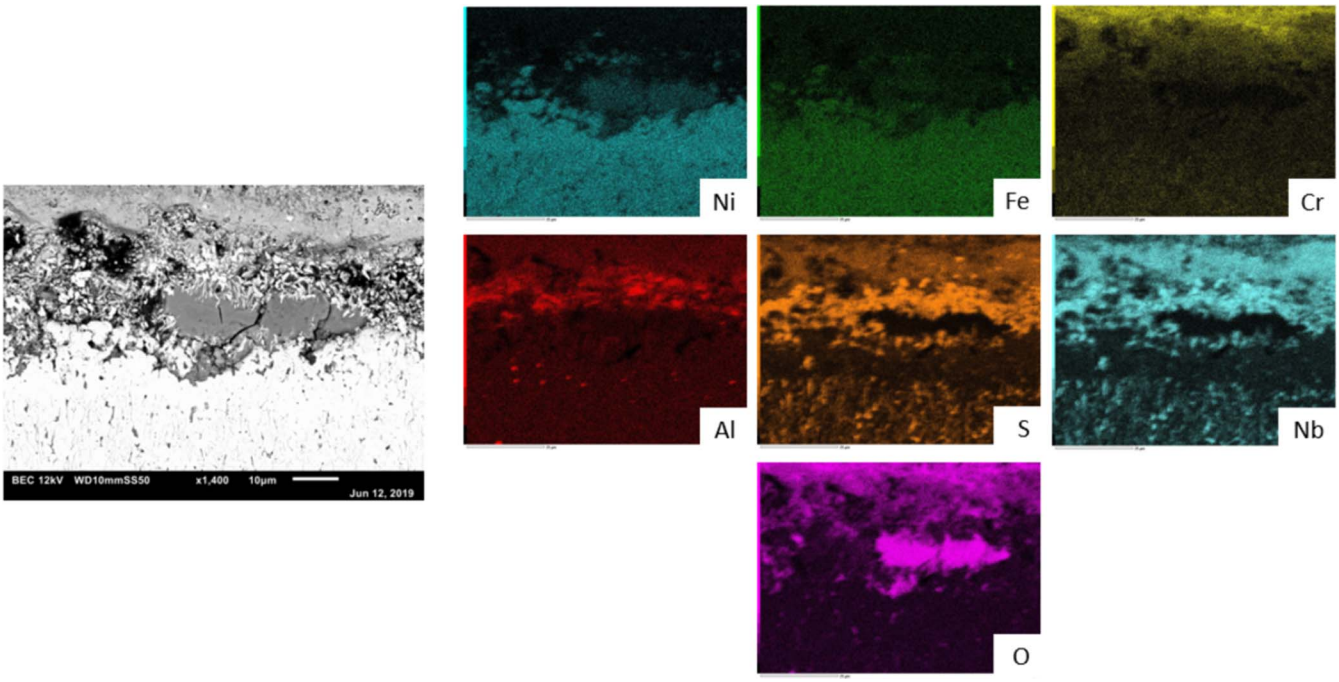

Figure 9. Higher magnification backscattered electron image and corresponding EDS elemental maps of the inner region shown in Figure 6.

form in Alloy 718,[15] leading to a chromium depletion zone beneath the chromia film. A depletion zone and the formation of sulfides was also observed in this study.

Conclusions

The corrosion behavior of $Al_{0.1}CoCrFeNi$ HEA and Alloy 718 in a molten Na_2SO_4-NaCl eutectic salt mixture at 750 ± 5°C was studied using electrochemical tests as well as scanning electron microscopy coupled with energy dispersive spectroscopy. The $Al_{0.1}CoCrFeNi$ HEA is less noble, has a higher polarization resistance and a lower corrosion rate relative to Alloy 718. The HEA forms an outer chromium oxide layer and an inner aluminum oxide layer while Alloy 718 forms only a single chromium oxide layer. The chromia layer is an effective deterrent to hot corrosion while the alumina scale is oxidation-resistant. This combination makes the $Al_{0.1}CoCrFeNi$ HEA more corrosion resistant than a conventional chromia former in environments typical of turbines. Therefore, this alloy appears to be a promising candidate for aerospace applications in light of the corrosion behavior displayed in this study.

Acknowledgments

The authors would like to acknowledge Prof. V. S. Raja (IIT Bombay) and Dr. J. C. Nava (Cal Poly Pomona) for detailed discussions. The authors would like to thank Steven Pierce, Dominic Dinh, Sam Bocker, Annette Wagner, Anan S. Hamdan, Joey Tulpinski and Ulus Ekerman (Cal Poly Pomona) for their support. The authors gratefully acknowledge financial support from Sylvia Hall, Dr. George and Mei Lai, the LA section of NACE International, Western States Corrosion Seminar, Western Area of NACE International, the NACE Foundation, the Kellogg Honors College, California Steel Industries Inc., and the Southern California Chapter of the Association for Iron & Steel Technology. The SEM images and EDS analyses were made possible through a NSF MRI grant DMR-1429674.

ORCID

R. S. Mishra https://orcid.org/0000-0002-1699-0614
J. C. Earthman https://orcid.org/0000-0002-5201-6456

References

1. Jien-Wei Yeh, Swe-Kai Chen, Su-Jien Lin, Jon-Yiew Gan, Tsung-Shune Chin, Tao-Tsung Shun, Chun-Huei Tsau, and Shou-Yi Chang, "Nanostructured High Entropy Alloys with Multiple Principal Elements: Novel Alloy Design Concepts and Outcomes," *Advanced Engineering Materials*, **6**(5), 299 (2004).
2. Ting Ting Zuo YongZhang, Zhi Tang, Michael C. Gao, Karin A. Dahmen, Peter K. Liaw, and Zhao Ping Lu, "Microstructures and Properties of High- Entropy Alloys," *Progress in Materials Science*, **61**, 1 (2014).
3. Yunzhu Shi, Bin Yang, and Peter K. Liaw, "Corrosion-Resistant High-Entropy Alloys: A Review," *Metals*, **7**, 33 (2017).
4. D. O. Svensson, "High Entropy Alloys: Breakthrough Materials for Aero Engine Applications," (Master's thesis, Chalmers University of Technology, 2014).
5. Te-Kang Tsao, An-Chou Yeh, Chen-Ming Kuo, and Hideyuki Murakami, "High Temperature Oxidation and Corrosion Properties of High Entropy Superalloys," *Entropy*, **18**, 1 (2016).
6. ASTM G59-97, "*Standard test method for Conducting Potentiodynamic Polarization Resistance Measurements*," West Conshohocken, PA: ASTM, 2014.
7. N. Perez, (2018). *Electrochemistry and Corrosion Science*, Springer, pg. 112.
8. R. G. Kelly et al. (2003). *Electrochemical Techniques in Corrosion Science and Engineering*, New York: Marcel Dekker. Pg 44.
9. "BT-Lab and EC-Lab Data Analysis and Processes," BioLogic Science Instruments. (2015). Pg 66.
10. Robert A. Rapp and Nobuo Otsuka, "The Role of Chromium in the Hot Corrosion of Metals," *ECS Transactions*, **16**(49), 271 (2009).
11. J. E. Croll and G. R. Wallwork, "The high-temperature oxidation of iron-chromium-nickel alloys containing 0–30% chromium", *Oxid Met*, **4**, 121 (1972).
12. Robert A. Rapp, "Chemistry and electrochemistry of hot corrosion of metals," *Materials Science Engineering*, **87**, 319 (1987).
13. F. S. Pettit, G. H. Meier et al. "*Oxidation and Hot Corrosion of Superalloys*," The Metal Society AIME, Warrendale, PA., 651 (1984).
14. G. S. Mahobia, N. Paulose, and V. Singh, "Hot Corrosion Behavior of Superalloy IN718 at 550 and 650°C" *Journal of Materials Engineering and Performance*, **22**(8), 2418 (2013).
15. J. L. Trinstancho-Reyes, M. Sanchez-Carrillo et al., "Electrochemical Impedance Spectroscopy Investigation of Alloy Inconel 718 in Molten Salts at High Temperature" *International Journal of Electrochemical Science*, **6**, 419 (2011).